JOURNAL OF PROPULSION AND POWER
Vol. 9, No. 4, July–Aug. 1993

Supersonic Turbomachine Rotor Flutter Control by Aerodynamic Detuning

Karen M. Spara* and Sanford Fleeter†
Purdue University, West Lafayette, Indiana 47907

A mathematical model is developed to analyze the flutter stability characteristics of an aerodynamically detuned rotor operating in a supersonic inlet flowfield with a supersonic axial component. Alternate-blade aerodynamic detuning is considered, accomplished by alternating the circumferential spacing of adjacent rotor blades. The unsteady aerodynamics are determined by developing an influence coefficient technique which is appropriate for both aerodynamically tuned and detuned rotor configurations. The effects of this detuning on the flutter stability characteristics of supersonic axial flow rotors are then demonstrated by applying this model to baseline 12-bladed rotors. Results show that, dependent on the specific blade row and flowfield geometry, alternate blade aerodynamic detuning is a viable flutter control mechanism for supersonic through-flow rotors.

Nomenclature

a	=	dimensionless perturbation sonic velocity
$C_{\alpha\alpha}$	=	torsion mode unsteady aerodynamic moment coefficient
$[CM]^n$	=	motion-induced influence coefficient of airfoil, n
c	=	airfoil chord
k	=	reduced frequency, $\omega c/U_\infty$
p	=	pressure
S	=	airfoil spacing
U_∞	=	cascade inlet velocity
u	=	dimensionless perturbation chordwise velocity
v	=	dimensionless perturbation normal velocity
x_0	=	elastic axis location measured from leading edge
α	=	amplitude of airfoil oscillations
β	=	interblade phase angle
β_d	=	detuned interblade phase angle
ε	=	aerodynamic detuning level

Introduction

THE development of supersonic axial flow compressors has long been of research interest due to the potential advantages of incorporating a supersonic through-flow fan into propulsion systems for high-speed vehicles. Breugelmans[1] performed the most thorough supersonic axial inlet rotor experiments utilizing an isolated rotor with a design inlet axial Mach number of 1.5. The rotor started and a total-to-total pressure ratio of about 2 at 80% design speed was attained. Also, the rotor appeared to be operating with an internal shock which produced subsonic axial flow out of the rotor. Unfortunately, this rotor suffered a blade failure before reaching the design point. As a result of this and other such major problems, the design of a successful supersonic axial flow compresser was considered to be too difficult. However, the current interest in high Mach number flight vehicles, coupled with recent developments in computational fluid dynamics, has renewed the research interest in supersonic axial flow fans.

Presented as Paper 89-2685 at the AIAA/ASME/SAE/ASEE 25th Joint Propulsion Conference, Monterey, CA, July 10–13, 1989; received Dec. 11, 1991; revision received Dec. 8, 1992; accepted Feb. 15, 1993. Copyright © 1993 by K. Spara and S. Fleeter. Published by the American Institute of Aeronautics and Astronautics, Inc., with permission.

*Thermal Sciences and Propulsion Center, School of Mechanical Engineering; currently member of technical staff, The Aerospace Corporation, Los Angeles, CA.

†Professor, School of Mechanical Engineering and Director, Thermal Sciences and Propulsion Center. Associate Fellow AIAA.

The successful development of a supersonic through-flow rotor requires the determination of the unsteady aerodynamics and flutter characteristics of supersonic axial flow blade rows. Previous experience with blade flutter has considered supersonic relative Mach numbers with subsonic, not supersonic, axial flow. Fortunately, a number of inviscid, oscillating flat plate cascade analyses appropriate for the supersonic axial flow regime have been developed. For example, Miles[2] addressed the problem of an oscillating airfoil in a supersonic flow within a wind tunnel. Lane[3] extended this model to include cascade effects. Gorelov,[4] Platzer and Chalkley,[5] and Nagashima and Whitehead[6] also considered the problem of an oscillating cascade in a supersonic axial flow. Kielb and Ramsey[7] developed a computer code based on Lane's theory and utilized it to investigate the effects on flutter of vibrational mode coupling, Mach number, structural damping, pitching axis location, stagger angle, and solidity. Their results showed that supersonic axial flow fan and compressor blades are susceptible to a strong torsional mode flutter having critical reduced frequencies which can be greater than one.

One approach to the control of flutter is structural detuning, defined as designed blade-to-blade differences in the natural frequencies of a blade row. Analyses have been developed which show that structural detuning enhances the flutter characteristics of a rotor. However, structural detuning is not a universally accepted passive aeroelastic control concept due to the associated manufacturing, material, inventory, and cost problems.[8]

Aerodynamic detuning, defined as designed passage-to-passage differences in the unsteady aerodynamics of a blade row, is a new approach for passive aeroelastic flutter control. It affects the fundamental driving mechanism for flutter, the unsteady aerodynamic loading on the individual airfoils. This results in the blading not responding in a classical traveling wave mode typical of a conventional aerodynamically tuned uniformly spaced rotor. For rotors operating in a supersonic inlet flowfield with a subsonic axial component, alternate blade circumferential spacing aerodynamic detuning has been shown to enhance both torsion and coupled bending-torsion mode flutter stability.[9,10]

In this article, a mathematical model is developed to analyze the effects of alternate blade aerodynamic detuning on the flutter characteristics of a rotor operating in a supersonic inlet flowfield with a supersonic axial flow component. As small changes in blade row solidity typically do not have a large effect on aerodynamic performance, the aerodynamic detuning is achieved by alternating the circumferential spacing of adjacent blades. The unsteady aerodynamics due to harmonic torsional airfoil oscillations are determined by developing an

influence coefficient technique which is appropriate for both aerodynamically tuned (uniformly spaced) and detuned rotors. The effects of this detuning on the flutter stability characteristics of supersonic axial flow rotor configurations are then demonstrated by applying this model to baseline 12-bladed rotors.

Unsteady Aerodynamic Model

The unsteady aerodynamics of a supersonic through-flow rotor are analyzed utilizing a strip theory approach, with the typical two-dimensional span section modeled as a cascade of flat plate airfoils at zero mean incidence. The cascade inlet flowfield is supersonic with a supersonic axial component, as schematically depicted in Fig. 1. It should be noted that disturbances cannot propagate upstream of the Mach lines. Thus, the flowfield in a particular passage is independent of the flow in adjacent passages.

Unsteady Flowfield

The fluid is assumed to be a perfect gas, with the flow inviscid, irrotational, adiabatic, and isentropic. The unsteady continuity and Euler equations are linearized by considering the unsteady flow to be small as compared to the steady flowfield. Following Platzer and Chalkley,[5] the method of characteristics is then used to transform the unsteady linearized differential equations into ordinary differential equations. Assuming harmonic time dependence, the dependent variables are the nondimensional chordwise, normal, and sonic perturbation velocities, u, v, and a, respectively

$$\frac{\partial u}{\partial x} + \sqrt{M_\infty^2 - 1}\frac{\partial v}{\partial y} + M_\infty^2\frac{\partial a}{\partial x} + ikM_\infty^2 a = 0 \quad (1a)$$

$$\frac{\partial u}{\partial x} + \frac{\partial a}{\partial x} + iku = 0 \quad (1b)$$

$$\frac{\partial u}{\partial y} - \sqrt{M_\infty^2 - 1}\frac{\partial v}{\partial x} = 0 \quad (1c)$$

where $k = \omega c/U_\infty$ is the reduced frequency.

Solutions to this system of partial differential equations are obtained by the method of characteristics. The characteristics are the Mach lines and streamlines:

right running Mach lines

$$\frac{dy}{dx} = \frac{1}{\sqrt{M_\infty^2 - 1}} \quad (2a)$$

left running Mach lines

$$\frac{dy}{dx} = \frac{-1}{\sqrt{M_\infty^2 - 1}} \quad (2b)$$

streamlines

$$\frac{dy}{dx} = 0 \quad (2c)$$

The compatibility equations, which are the ordinary differential equations that act along the characteristics, are given in Eq. (3).

$$\left(\frac{\partial u}{\partial x}\right)_\xi - \left(\frac{\partial v}{\partial x}\right)_\xi + ik\frac{M_\infty^2}{M_\infty^2 - 1}(u - a) = 0 \quad (3a)$$

$$\left(\frac{\partial u}{\partial x}\right)_\eta + \left(\frac{\partial v}{\partial x}\right)_\eta + ik\frac{M_\infty^2}{M_\infty^2 - 1}(u - a) = 0 \quad (3b)$$

$$\left(\frac{\partial u}{\partial x}\right)_{str} + \left(\frac{\partial a}{\partial x}\right)_{str} + iku = 0 \quad (3c)$$

where the subscripts ξ, η, and str indicate that the relation is valid along the right or left running Mach lines or the streamline direction, respectively.

The flow tangency boundary condition requires that v is equal to the normal velocity of the airfoil surfaces on the mean airfoil position. For a cascade undergoing harmonic torsional motion about an elastic axis located at x_0, as measured from the leading edge, the flow tangency boundary condition on the nth airfoil in the cascade is given in Eq. (4)

$$[v_n(x, y_s, t)/U_\infty] = -\alpha[1 + (x - x_0)ik]e^{i(kt + n\beta)} \quad (4)$$

where y_s is the mean position of the nth airfoil.

The formulation of the basic unsteady aerodynamic mathematical model is now complete. For the uniformly spaced tuned cascade, finite differences have been used to solve the system of three differential equations in three unknowns, Eq. (3), at the intersection of the characteristics for the u, v, and a velocities, subject to the boundary condition given in Eq. (4). The unsteady perturbation pressure on the surfaces of a reference airfoil are then determined from the perturbation sonic velocity. Finally, the nondimensional unsteady aerodynamic lift and moment, L and M, and the standard $C_{\alpha\alpha}$ are calculated as follows:

$$L = \int_0^1 \Delta p(x, y_s, t)\, dx \quad (5a)$$

$$M = \int_0^1 \Delta p(x, y_s, t)(x - x_0)\, dx = C_{\alpha\alpha}\alpha e^{i\omega t} \quad (5b)$$

where Δp denotes the nondimensional pressure difference across the chordline of a reference airfoil.

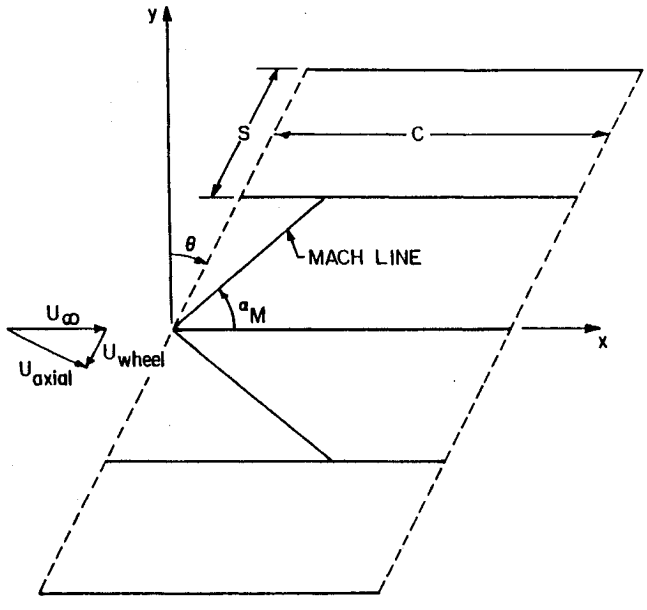

Fig. 1 Flat plate airfoil cascade in a supersonic inlet flow with a supersonic axial component.

Aerodynamically Detuned Cascade

Alternate blade circumferential spacing aerodynamic detuning is being considered. Introducing this detuning into the baseline tuned cascade results in two reference passages: 1) an increased spacing or decreased solidity passage, and 2) a decreased spacing or increased solidity passage. Also, there are two reference airfoils for each passage, denoted by R_0

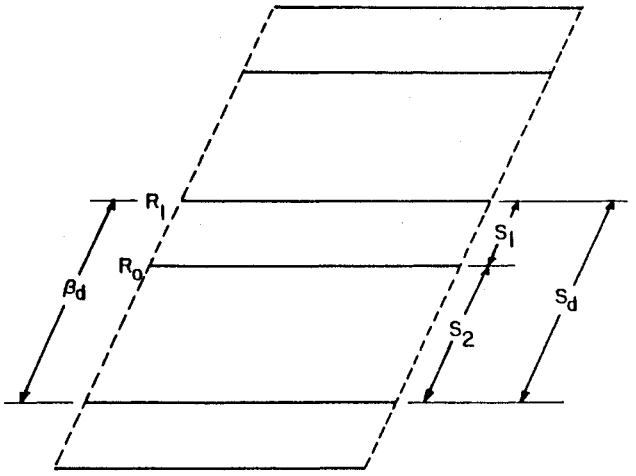

Fig. 2 Aerodynamically detuned cascade geometry.

and R_1. The aerodynamically detuned airfoil cascade can be considered as being comprised of two uniformly spaced cascades, each having a spacing S_d which is twice that of the baseline cascade (Fig. 2). The circumferential spacing between adjacent airfoils, S_1 and S_2, is specified by ε

$$S_{2,1} = (1 \pm \varepsilon)S \tag{6}$$

where S is the spacing of the baseline cascade, and S_1 and S_2 are the spacings of the detuned cascade.

An interblade phase angle for the aerodynamically detuned cascade configuration can be defined. In particular, each set of airfoils is individually assumed to be executing harmonic torsional oscillations with a constant aerodynamically detuned β_d between adjacent airfoils of each set (Fig. 2). Therefore, this detuned cascade interblade phase angle is twice that for the corresponding baseline-tuned cascade

$$\beta_d = 2\beta \tag{7}$$

where β is the baseline-tuned cascade.

For a rotor with N uniformly spaced blades, Lane[11] showed that the values of β must satisfy Eq. (8). For the aerodynamically detuned cascade, the interblade phase angles between adjacent airfoils for flutter are unknown

$$\beta = \frac{2\pi r}{N}, \quad r = 0, \pm 1, \pm 2, \ldots, \pm N - 1 \tag{8}$$

where + and − refer to the forward and backward traveling waves, respectively.

The previously described general method of characteristics solution procedure for the perturbation velocity components is then applied to the two passages of the aerodynamically detuned cascade. However, the boundary condition given in Eq. (4) requires that the blades oscillate at equal amplitudes. Also, the β between adjacent blades must be specified. Neither of these requirements is appropriate for the aerodynamically detuned cascade. These limitations are overcome by developing and utilizing an unsteady aerodynamic influence coefficient technique to predict the cascade unsteady aerodynamic loading.

Influence Coefficients

For torsion mode flutter, only the oscillating cascade unsteady aerodynamics need be considered. For this case, the unsteady aerodynamic moments acting on the two reference airfoils of the detuned cascade, R_0 and R_1, are written in terms of influence coefficients in Eq. (9)

$$M_{R_0,R_1} = ([CM]^0_{R_0,R_1}\bar{\alpha}_{R_0} + [CM]^1_{R_0,R_1}\bar{\alpha}_{R_1})e^{i\omega t} \tag{9}$$

where the double subscripts express two equations, one for each reference airfoil R_0 and R_1; $\bar{\alpha}_{R_0,R_1}$ are the complex displacements of the reference airfoils; and $[CM]$ denotes the motion-induced influence coefficients.

To determine the influence coefficients $[CM]$, the unsteady aerodynamic model for the two-reference passage detuned cascade is utilized directly with the modification of the airfoil surface boundary conditions on the two reference airfoils. The influence coefficients $[CM]^0_{R_0,R_1}$ and $[CM]^1_{R_0,R_1}$ are the unsteady aerodynamic moments acting on the two reference airfoils and are determined by analyzing the two reference flow passages with appropriate modifications to the boundary conditions of the two reference airfoils. $[CM]^0_{R_0,R_1}$ are calculated by considering a unit amplitude motion of only the reference airfoil R_0, with β_d specified and reference airfoil R_1 stationary. The influence coefficients $[CM]^1_{R_0,R_1}$ are obtained in an analogous manner, but with a unit amplitude motion of only R_1 and R_0, stationary.

To investigate the effects of aerodynamic detuning on torsion mode flutter, the stability of the cascade is determined by writing the influence coefficients in the following matrix form:

$$\begin{bmatrix} M_{R_0} \\ M_{R_1} \end{bmatrix} = \begin{bmatrix} [CM]^0_{R_0} - C_{\alpha\alpha} & [CM]^1_{R_0} \\ [CM]^0_{R_1} & [CM]^1_{R_1} - C_{\alpha\alpha} \end{bmatrix} \begin{bmatrix} \bar{\alpha}_0 \\ \bar{\alpha}_1 \end{bmatrix} \begin{bmatrix} 0 \\ 0 \end{bmatrix} \tag{10}$$

Equation (10) defines a classical eigenvalue problem. The eigenvalue represents $C_{\alpha\alpha}$ with the eigenvectors defining the phase angle between adjacent oscillating airfoils. β_d must be specified. The permissible values of β_d are obtained from Eq. (8) by setting N equal to the number of blades on the baseline uniformly spaced rotor. In this study, 12-bladed baseline rotors are considered. All permissible interblade phase angles must be utilized to find the least stable response mode. Also, Eq. (10) represents two equations, therefore, two eigenvalues are determined for each β_d. The stability of the baseline or aerodynamically detuned cascade is specified by the sign of the imaginary part of $C_{\alpha\alpha}$. When the sign is negative, the motion of the airfoils is damped and the cascade is stable. Conversely, when the sign is positive, the motion of the airfoils increases and the cascade is unstable.

Model Verification

To verify the validity of this unsteady aerodynamic cascade model and the influence coefficient technique, predictions of

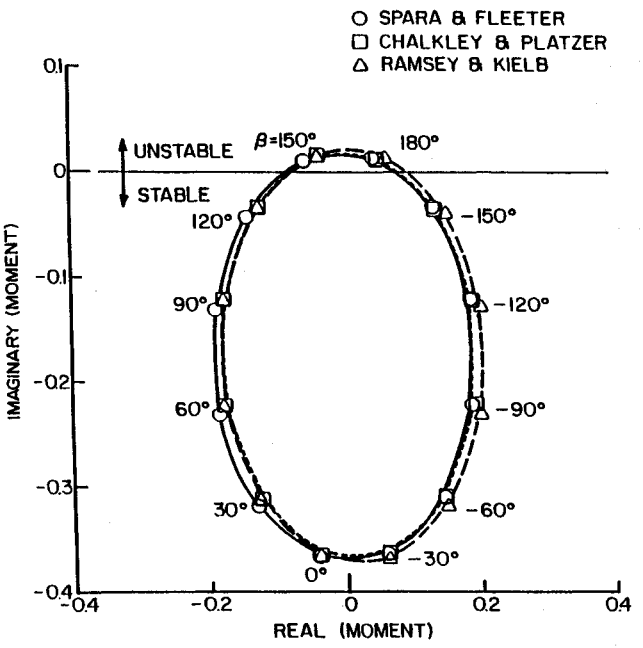

Fig. 3 Oscillating cascade model verification.

the oscillating cascade unsteady aerodynamics for a conventional tuned cascade representation of a 12-bladed rotor are compared to analogous predictions from the unsteady aerodynamic models of Platzer and Chalkley[5] and Kielb and Ramsey.[7] A study was conducted to determine the number of grid points necessary to obtain an accurate prediction, with 600 grid points used for this analysis.

Figure 3 shows the verification of the oscillating cascade model. The real and imaginary parts of the unsteady aerodynamic moment coefficient are plotted with the tuned β as a parameter. The excellent agreement between all three analyses is readily apparent.

Results

The effects of alternate blade aerodynamic detuning on the flutter characteristics of a rotor operating in a supersonic inlet flowfield with a supersonic axial flow component are now demonstrated. This is accomplished by applying this model to three baseline 12-bladed supersonic rotors with fundamentally different flow geometries.

Baseline

With a supersonic inlet flowfield, waves of finite strength originate from the leading and trailing edges of the airfoils in the cascade representing the flow geometry of the rotor. Also, if the axial velocity component is supersonic, the airfoil trailing-edge waves are always downstream of the other airfoils. However, the airfoil leading-edge waves may be reflected from the surfaces of adjacent airfoils. Three such cascade flow geometries are of interest here. They are termed cascade F, cascade G, and cascade K. As schematically depicted in Fig. 4, cascade F has one airfoil leading-edge wave reflection, whereas cascades G and K each have one reflection of both of the airfoil leading-edge waves. The parameters which define these cascade geometries are presented in Table 1.

To investigate the effect of the various detuning mechanisms on torsion mode flutter, a reduced frequency for each

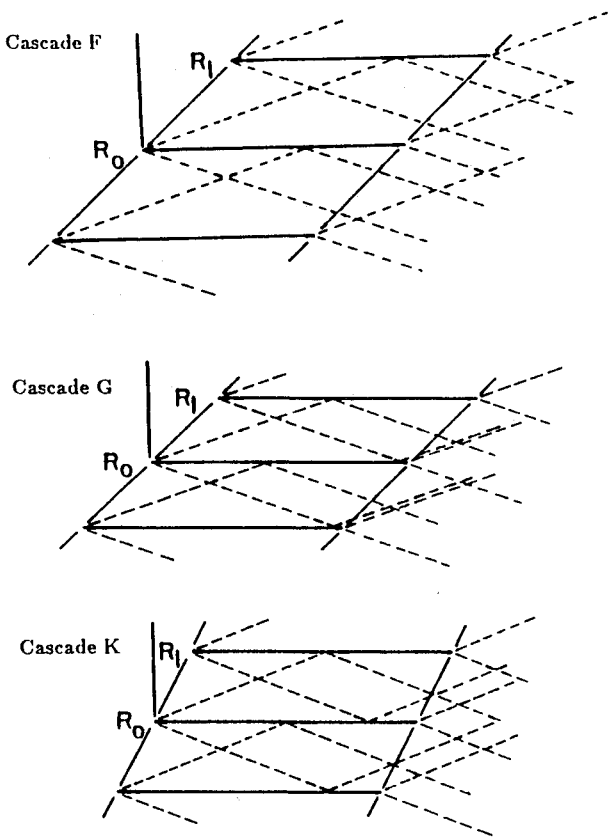

Fig. 4 Baseline cascade flow geometries.

Table 1 Cascade parameters

Cascade	Inlet Mach number	Stagger angle	Solidity	Elastic axis, % chord
F	3	45 deg	2	50
G	3	45 deg	2.7778	50
K	2.606	28 deg	3.215	50

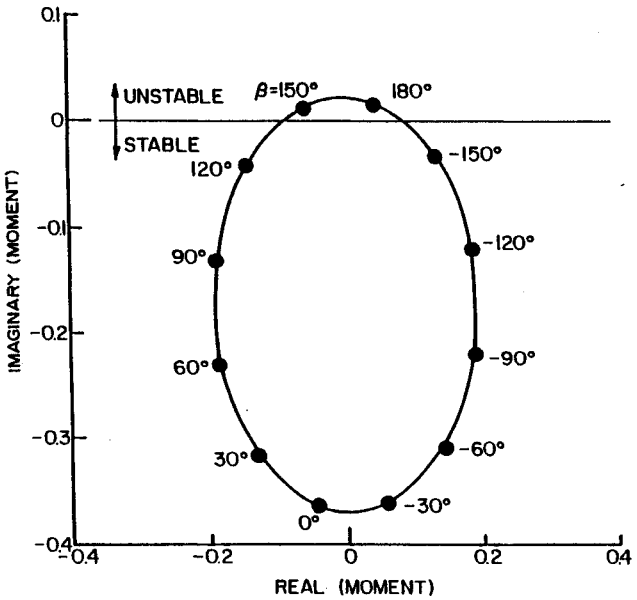

Fig. 5 Torsional stability of baseline cascade F rotor.

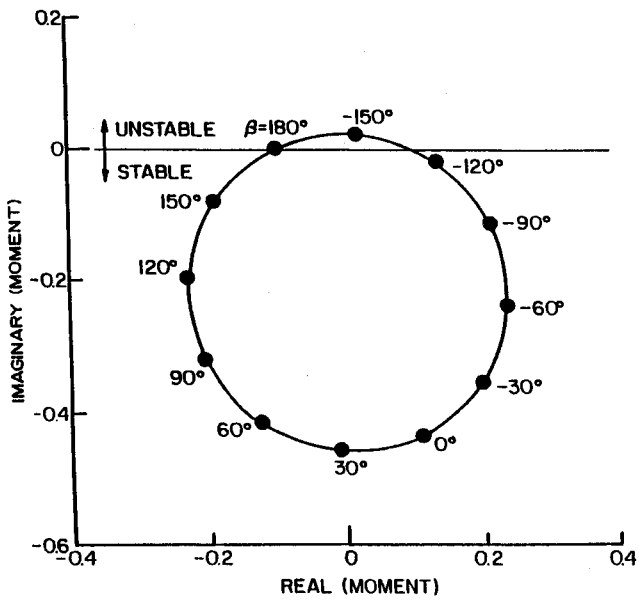

Fig. 6 Torsional stability of baseline cascade G rotor.

cascade configuration is selected such that each baseline uniformly spaced 12-bladed rotor is unstable. Each of these rotors is then aerodynamically detuned, with the stability of these detuned rotor configurations then determined.

The stability of the baseline cascades F and G rotors with reduced frequencies of 1.3 and 1.2, respectively, and the cascade K rotor with a reduced frequency of 0.7 are presented in Figs. 5–7. Cascade F is unstable for β equal to 180 and 150 deg, cascade G for β of 180 and -150 deg, and cascade K for β of -150 and -120 deg.

Aerodynamic Detuning

Three alternate circumferential spacing, aerodynamically detuned configurations of each cascade geometry are consid-

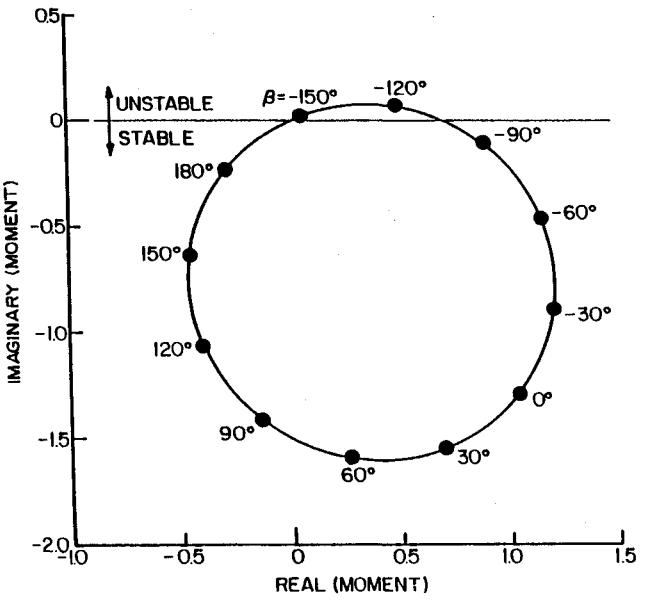

Fig. 7 Torsional stability of baseline cascade K rotor.

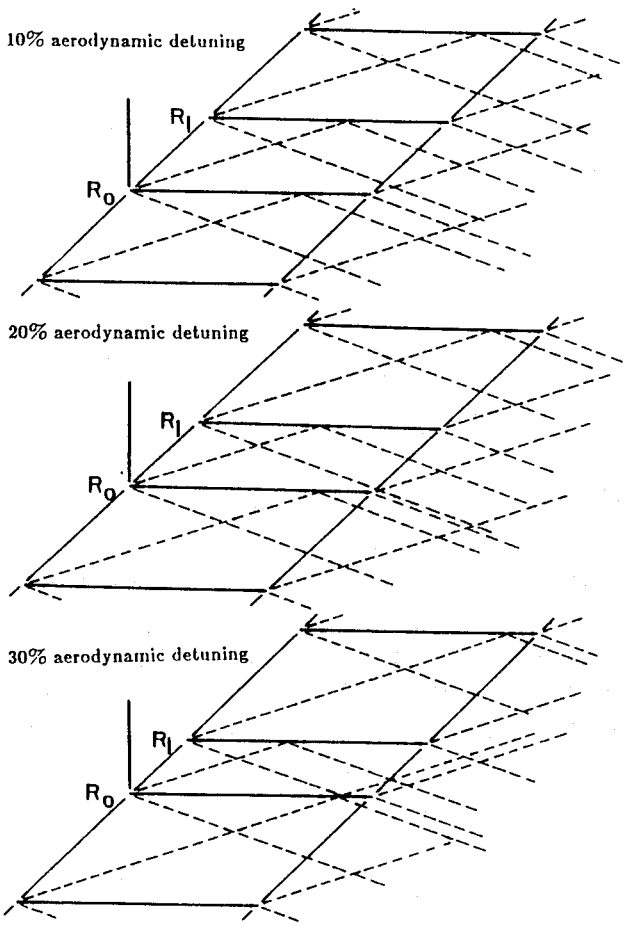

Fig. 8 Aerodynamically detuned cascade F flow geometries.

ered: 10, 20, and 30% detuning. The flowfield wave structure for these configurations are depicted in Figs. 8–10 for cascades F, G, and K, respectively.

For cascade F, as the level of aerodynamic detuning is increased, the wave reflection on the pressure surface of R_1 moves toward the leading edge, whereas the pressure surface reflection on R_0 moves toward the trailing edge. The left running Mach wave from the leading edge of R_1 does

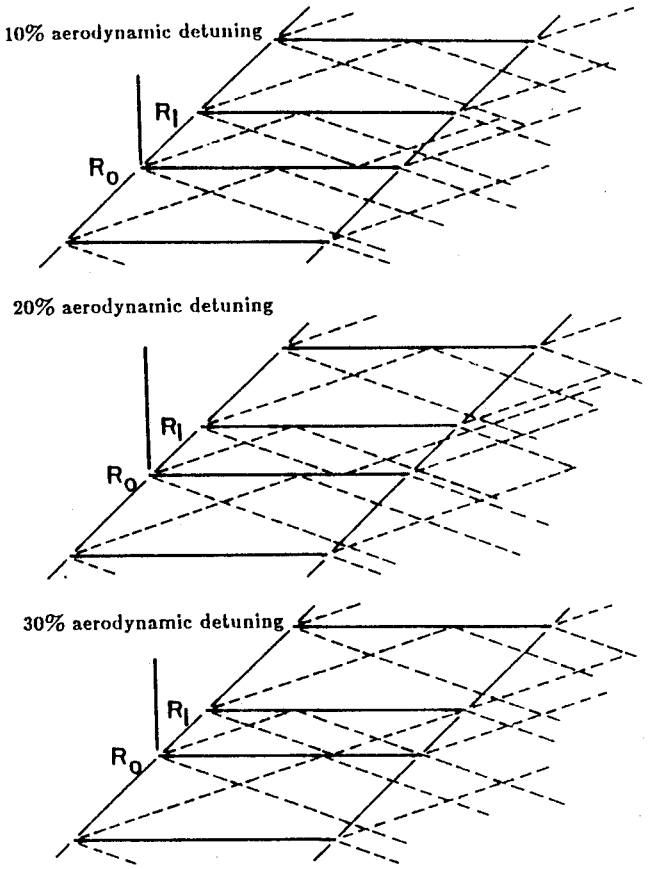

Fig. 9 Aerodynamically detuned cascade G flow geometries.

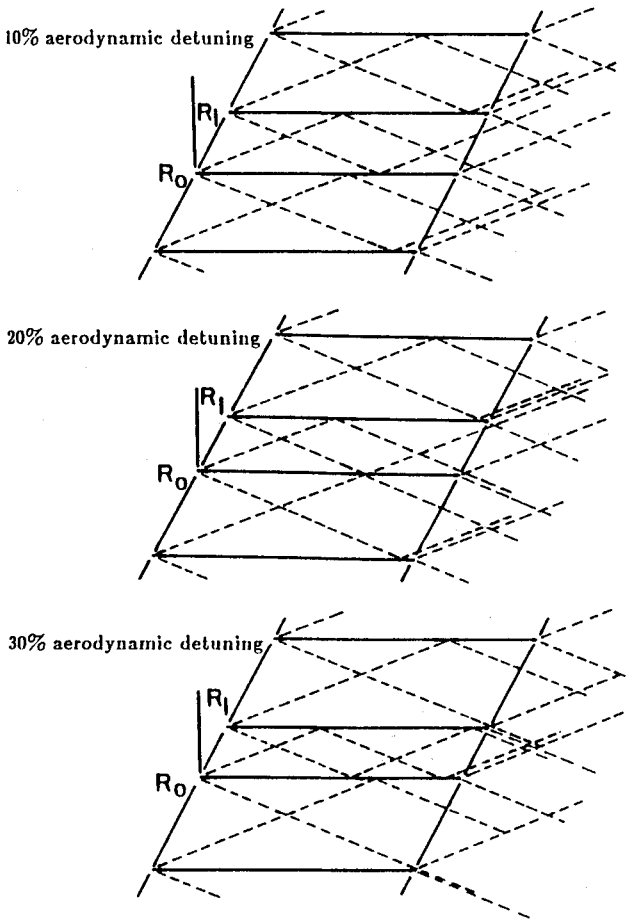

Fig. 10 Aerodynamically detuned cascade K flow geometries.

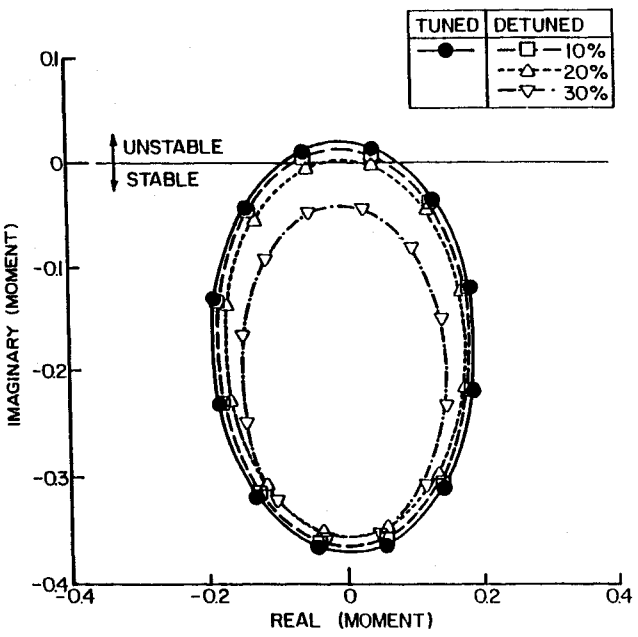

Fig. 11 Stability of aerodynamically detuned cascade F rotors.

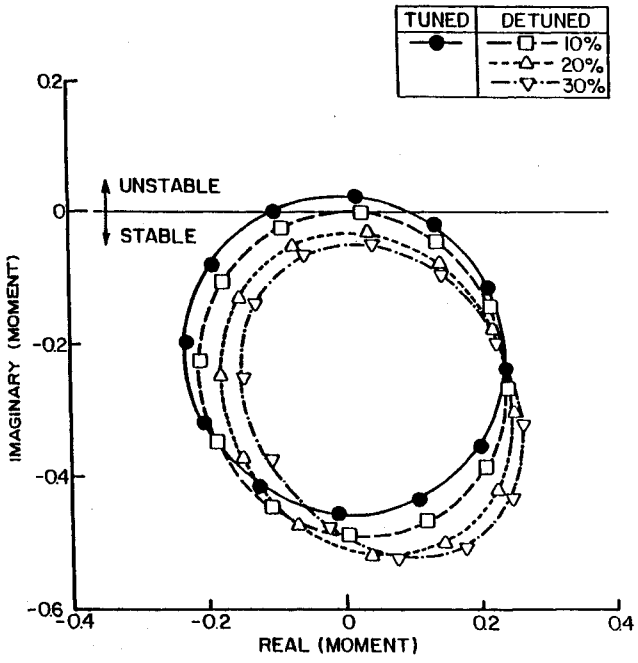

Fig. 12 Stability of aerodynamically detuned cascade G rotors.

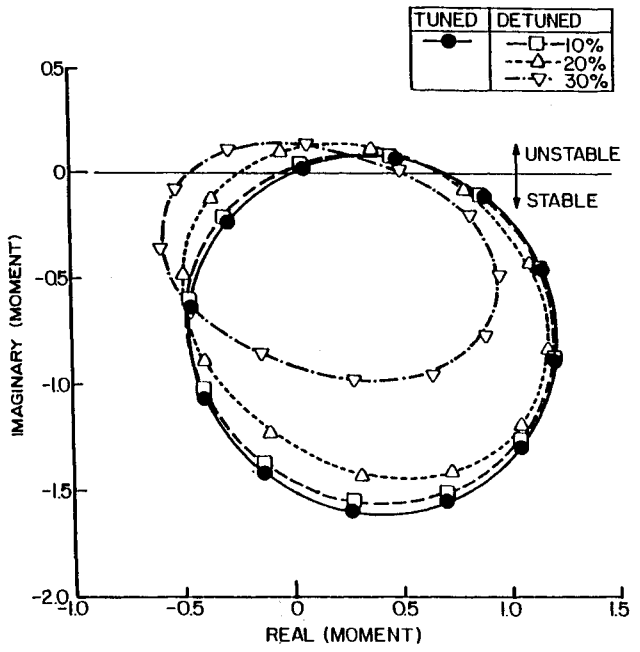

Fig. 13 Stability of aerodynamically detuned cascade K rotors.

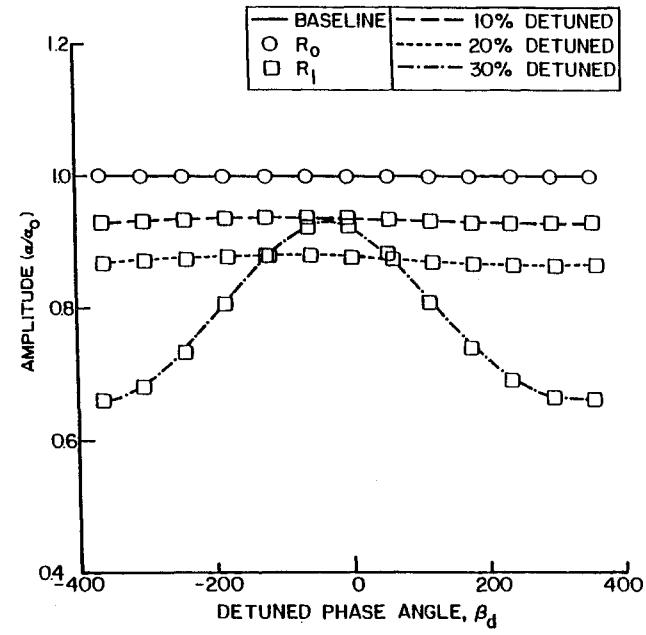

Fig. 14 Effect of aerodynamic detuning on the amplitude of blade response for cascade F.

not intersect R_0 for the baseline, 10 or 10% detuning. However, with 30% detuning, it intersects the suction surface of airfoil R_0.

For cascade G, as the level of aerodynamic detuning is increased, the wave reflection on the pressure surface of R_1 also moves toward the leading edge, while the wave reflection on the pressure surface of R_0 moves toward the trailing edge. The left running Mach line from the leading edge of R_1 intersects the suction surface of R_0 for all levels of aerodynamic detuning, and moves toward the leading edge as the level of aerodynamic detuning is increased.

The same trend is evident for cascade K as in cascade G for the pressure surfaces of R_1 and R_0: with increased levels of aerodynamic detuning, the Mach wave reflection moves toward the leading edge for R_1, but toward the trailing edge for R_0. The left running Mach line from the leading edge of R_0 intersects the suction surface of R_1 with 10 and 20% aerodynamic detuning, and moves toward the trailing edge as the level of aerodynamic detuning increases. With 30% aerodynamic detuning, the Mach line does not intersect the suction surface of blade R_1. The left running Mach line from the leading edge of R_1 intersects the suction surface of blade R_0 for all levels of detuning and moves toward the leading edge as the level of aerodynamic detuning is increased.

Alternate spacing aerodynamic detuning enhances the torsion mode stability of the baseline cascade F and G rotors, but decreases the stability of the cascade K rotor, as shown in Figs. 11–13. In particular, incorporating 10% aerodynamic detuning into cascade F increased stability, but the detuned rotor is still unstable. Cascade F with 20% and cascade G with 10% aerodynamic detuning are neutrally stable. The introduction of 30% aerodynamic detuning into cascade F and either 20 or 30% detuning into cascade G results in stable rotor configurations. In contrast, this alternate spacing aerodynamic detuning does not enhance the cascade K rotor stability. In fact, as the level of aerodynamic detuning increases, the cascade K rotor becomes unstable for more interblade phase angle values.

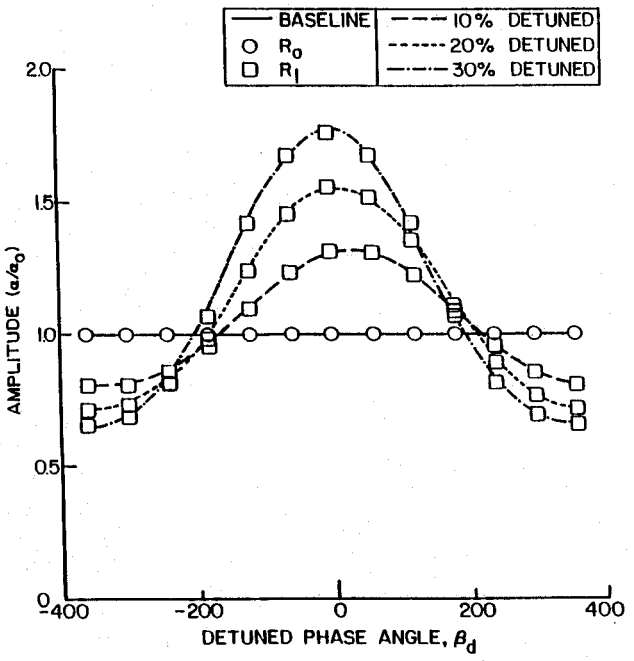

Fig. 15 Effect of aerodynamic detuning on the response interblade phase angle of cascade G.

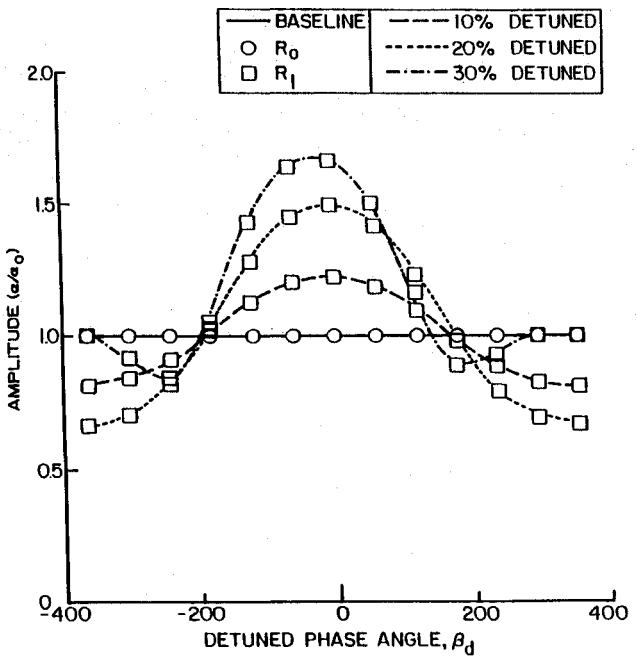

Fig. 16 Effect of aerodynamic detuning on the amplitude of blade response for cascade K.

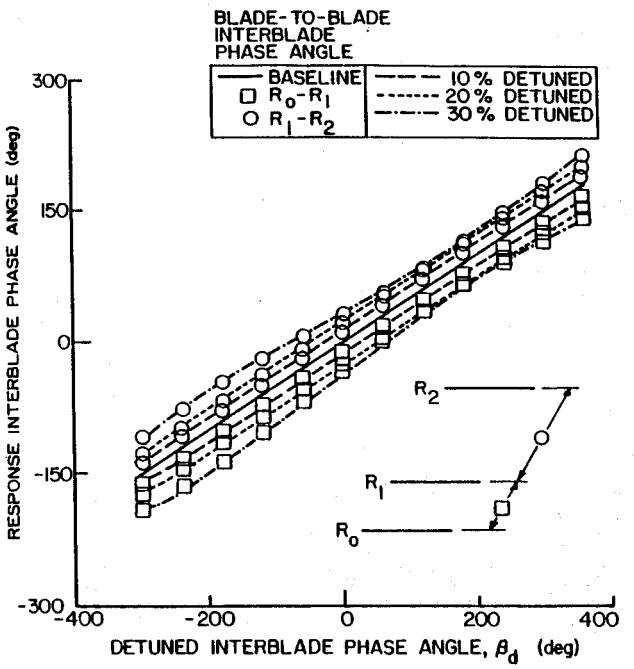

Fig. 17 Effect of aerodynamic detuning on the response interblade phase angle of cascade F.

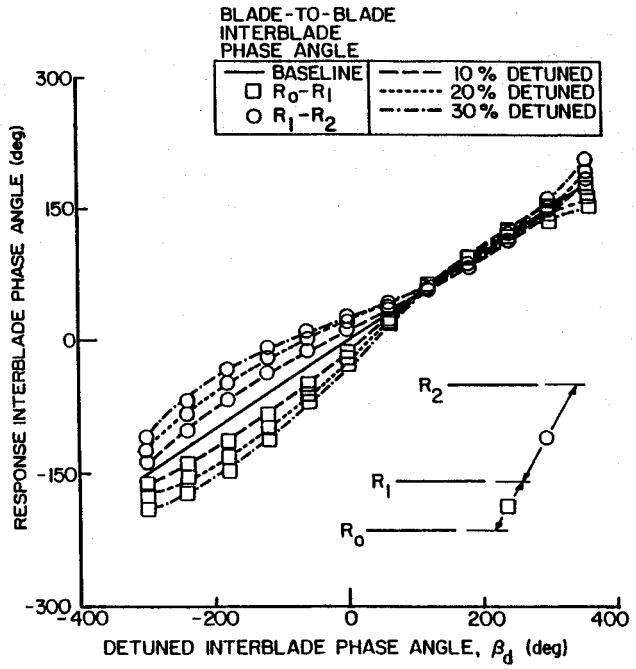

Fig. 18 Effect of aerodynamic detuning on the response interblade phase angle of cascade G.

The effects of aerodynamic detuning on the equal amplitude, constant interblade phase angle, and vibratory responses of the three baseline rotors are shown in Figs. 14–19. In particular, these figures show the effect of aerodynamic detuning on the amplitude and interblade phase angle of the vibratory response of the cascade F, G, and K rotors as a function of the detuned β_d. Thus, the response in a particular vibration mode corresponds to a particular value of β_d. Also, for each cascade configuration, R_0 has been assumed to have a unit amplitude of response.

For cascade F, the amplitude of response of R_1 decreases with increased detuning for 10 and 20% aerodynamic detuning, with this response nearly independent of the detuned interblade phase angle value. However, for 30% detuning, although the amplitude of response of airfoil R_1 is decreased, the decreased amplitude is highly dependent on the detuned interblade phase angle value. Namely, R_1 has a maximum response for detuned interblade phase angle values near zero, with the response decreasing for both forward and backward traveling waves achieving a minimum for detuned interblade phase angles of 300 and ±360 deg, i.e., minimal response for tuned interblade phase angles of 150 and 180 deg which are the unstable interblade phase angles of the baseline rotor.

For the cascade G and K rotors, the amplitude of response of R_1 is a function of β_d for all levels of aerodynamic detuning. For detuned interblade phase angles in the approximate ranges of −180 to −360 and 180 to 360 deg, the response amplitudes of R_1 are smaller than those of R_0, analogous to the cascade F results. However, in contrast to cascade F, the response amplitudes of R_1 are greater than those of R_0 for detuned interblade phase angles between approximately +180 and −180 deg.

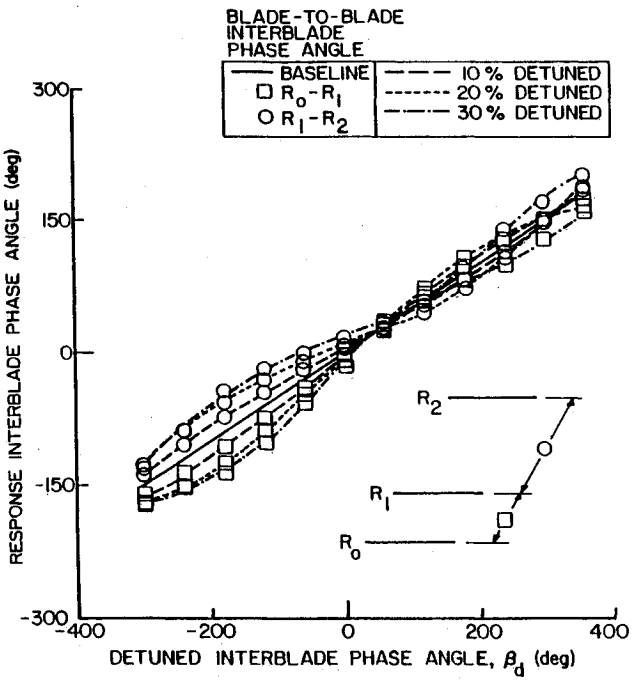

Fig. 19 Effect of aerodynamic detuning on the response interblade phase angle of cascade K.

The response phase angles for the cascade F detuned rotor configurations are a function of the level of aerodynamic detuning and, analogous to the baseline uniformly spaced rotor, vary in a nearly linear fashion with detuned interblade phase angle value. For the cascade G and K rotors, however, the response interblade phase angles, although a function of the aerodynamic detuning level, do not vary linearly with the detuned interblade phase angle. Rather, aerodynamic detuning has a larger effect on the response phase for negative detuned interblade phase angle values than for positive ones, i.e., a larger effect for backward traveling waves. Also, for all three baseline rotors, it should be noted that the geometry of the aerodynamically detuned cascades do not define the detuned cascade response phase angles, e.g., 30% aerodynamic detuning does not result in a 30% difference in the interblade phase angles for the two passages of the detuned cascade.

Summary and Conclusions

A mathematical model has been developed to analyze the effects of aerodynamic detuning on the flutter of a rotor operating in a supersonic inlet flowfield with a supersonic axial component. The aerodynamic detuning was achieved by alternating the circumferential spacing of adjacent blades. The unsteady aerodynamics due to harmonic torsional airfoil oscillations were determined by developing an influence coefficient technique appropriate for both aerodynamically tuned (uniformly spaced) and detuned rotor configurations.

The effects of this detuning on the flutter characteristics of a supersonic axial flow rotor were then demonstrated by applying this model to three baseline 12-bladed rotors with flow geometries denoted by cascades F, G, and K. Aerodynamic detuning was found to increase the stability of cascades F and G. For cascade K, however, this detuning resulted in decreased stability. Thus, dependent on the specific blade row and flowfield geometry, aerodynamic detuning is a viable passive flutter control technique for supersonic through-flow rotors.

References

[1]Breugelmans, F. A. E., "The Supersonic Axial Inlet Component in a Compressor," American Society of Mechanical Engineers Paper 75-GT-26, March 1975.

[2]Miles, J. W., "The Compressible Flow Past an Oscillating Airfoil in a Wind Tunnel," *Journal of the Aeronautical Sciences*, Vol. 23, No. 7, 1956, pp. 671–678.

[3]Lane, F., "Supersonic Flow Past an Oscillating Cascade with Supersonic Leading-Edge Locus," *Journal of the Aeronautical Sciences*, Vol. 24, Jan. 1957, pp. 65, 66.

[4]Gorelov, D. N., "Lattice of Plates in an Unsteady Supersonic Flow," *Fluid Dynamics*, Vol. 1, No. 4, 1966, pp. 34–39.

[5]Platzer, M. F., and Chalkley, H. G., "Theoretical Investigation of Supersonic Cascade Flutter and Related Interference Problems," AIAA/ASME/SAE 13th Structures, Structural Dynamics, and Materials Conf., AIAA Paper 72-377, San Antonio, TX, April 10–12, 1972.

[6]Nagashima, T., and Whitehead, D. S., "The Linearized Supersonic Unsteady Flow in Cascades," *ARC-R and M-3811, Aeronautics Research Council*, London, 1977.

[7]Kielb, R. E., and Ramsey, J. K., "Flutter of a Fan Blade in Supersonic Axial Flow," American Society of Mechanical Engineers Paper 88-GT-78, June 1988.

[8]Crawley, E. F., and Hall, K. C., "Optimization and Mechanisms of Mistuning of Cascades," American Society of Mechanical Engineers Paper 84-GT-196, 1984.

[9]Hoyniak, D., and Fleeter, S., "Aerodynamic Detuning Analysis of an Unstalled Supersonic Turbofan Cascade," American Society of Mechanical Engineers Paper 85-GT-192, March 1985.

[10]Hoyniak, D., and Fleeter, S., "The Effect of Circumferential Aerodynamic Detuning on Coupled Bending-Torsion Unstalled Supersonic Flutter," *Journal of Turbomachinery*, Vol. 108, No. 2, 1988, pp. 253–260.